19th Australasian Fluid Mechanics Conference
Melbourne, Australia
8-11 December 2014

Cavitation About a Sphere Impacting a Flat Surface

K. L. de Graaf, P. A. Brandner, J. Y. Lee and B. W. Pearce

Australian Maritime College,
University of Tasmania, Launceston, Tasmania 7250, Australia

Abstract

Cavitation occurring when a spherical body impacts, and rebounds from, a flat surface has been investigated experimentally using high-speed photography. This phenomenon occurs in nature with the mantis shrimp utilising both the initial physical impact and also the shockwave impulse from the associated cavitation bubble collapse, to break open the shell of its prey. A 45 mm Ertacetal® plastic sphere attached to a thin rod was fitted to a spring-loaded mechanism which allowed for the impact velocity of the sphere to be varied (up to 3.2 m/s). Experiments were performed in quiescent water at static pressures of 40 to 140 kPa and equilibrium saturation condition. The sphere velocity and acceleration, and cavitation bubble radius and interface velocity were determined from the high-speed images which were acquired at a frame rate of 100 kHz. A power law relationship was found between the maximum bubble radius, non-dimensionalised on sphere radius, and the pressure, non-dimensionalised to a cavitation number, for the range of velocities and pressures investigated.

Introduction

The cavitation induced when a sphere impacts a solid surface has been studied in various forms. Joseph [2] proposed the possibility of cavitation induced by shear stress. Marston *et al.* [5] found cavitation to form on the rebound of a sphere from a surface (filmed at 20 kHz) and favourably compared their experimental results with the theoretical stress limits proposed by Joseph. Seddon *et al.* [8] presented experimental results of the formation of shear-stress-induced vapour cavities during the approach of a sphere on a solid boundary. High-speed images were taken at 10 kHz and showed the presence of cavitation as the sphere moved toward the boundary. Mansoor *et al.* [4] used high-speed photography (at 33 kHz) to film the cavitation made by a tungsten-carbide sphere dropped onto a glass surface covered in a layer of Newtonian fluid. The cavitation was seen to form only after impact.

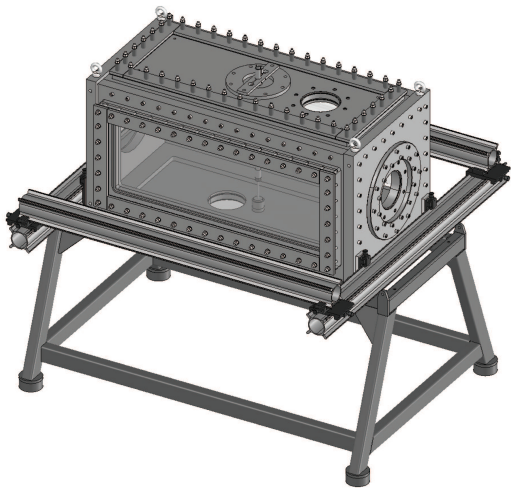

Figure 1. The variable-pressure Bubble Dynamics Chamber has a test volume of 520×520×1200 mm. The short ends and two opposite long sides (top and bottom) are stainless steel plate. The remaining sides are 85 mm thick acrylic windows. The chamber can be operated at pressures from 10 to 400 kPa.

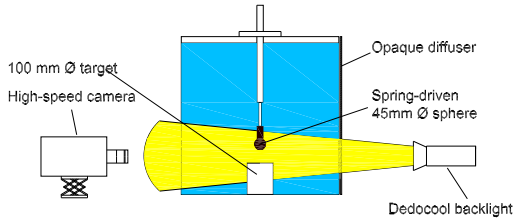

Figure 2. Schematic of the experimental setup showing location of sphere, target, high-speed camera, diffuser and backlight. The compression spring to accelerate sphere is housed within the sphere-tube assembly and not shown.

The formation of cavitation due to impact forces occurs in nature with the example of the peacock mantis shrimp (*Odontodactylus scyllarus*) striking prey with a raptorial appendage. The bubble formed behaves as a typical vapour bubble according to the Rayleigh-Plesset equation [1], and undergoes multiple rebounds with corresponding pressure field changes. The strike can generate forces up to 1501 N [6] at peak speeds of 14 to 23 m/s [7]. Another example is the snapping shrimp (*Alpheus heterochaelis*) which generates a sonoluminescing cavitation bubble when its snapper claw snaps shut [3].

The investigations discussed above used a sphere falling under gravity. To generate higher velocities representative of those exhibited by the mantis shrimp, the experiments presented here use a spring-loaded mechanism to accelerate the sphere. The maximum radius of the bubble generated between the sphere and the impact surface has been measured using high speed photography. The effect on the bubble size of static pressure and impact velocity is investigated.

Experimental Setup

The experiments were performed in the variable-pressure Bubble Dynamics Chamber (BDC) at the Cavitation Research Laboratory, University of Tasmania. The chamber, shown in figure 1, is constructed of 46 mm thick stainless steel plates and sits horizontally on one long side with a stainless steel plate top and bottom. Two opposite long sides have 85 mm acrylic windows, and the short ends are both stainless steel plate. The chamber has a test volume of 520×520×1200 mm filled with distilled water and a smaller plenum of air (not shown) attached to the top through which the pressurising system is implemented. The pressure in the tank is controlled with an automated system between 10 to 400 kPa.

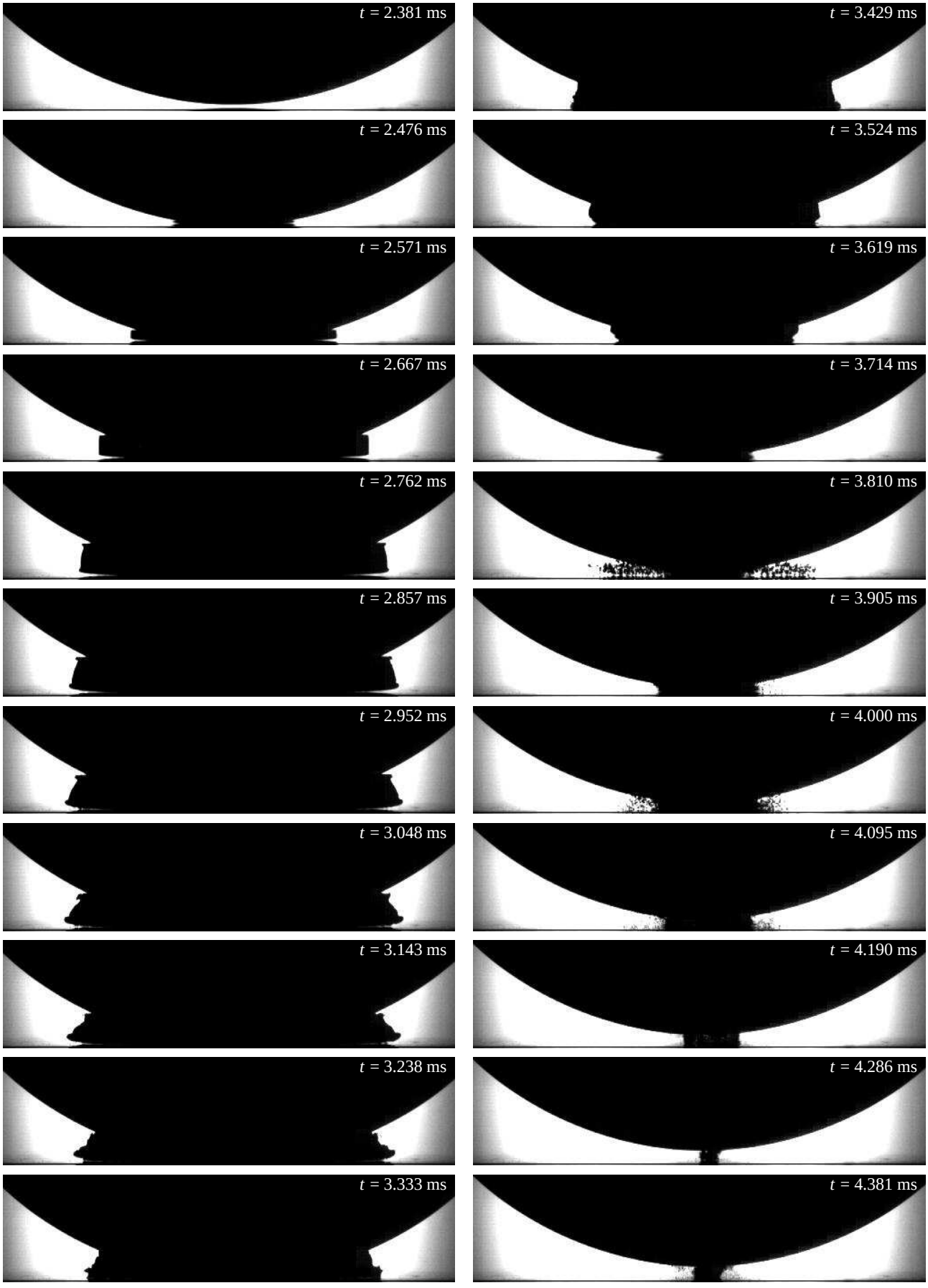

Figure 3. Continued over page.

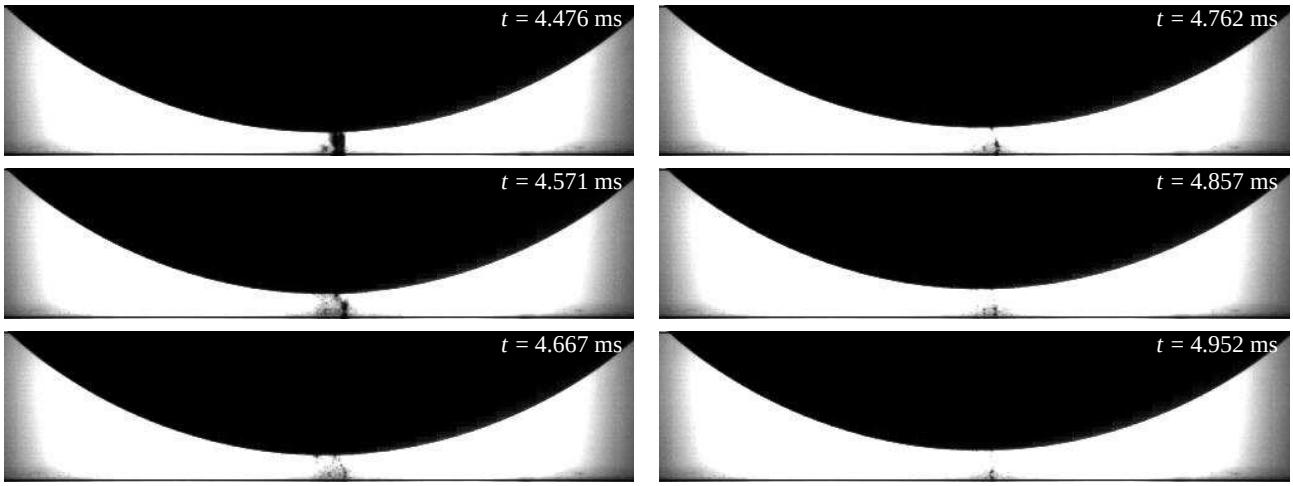

Figure 3. High-speed shadow photography images taken at 105 kHz showing cavitation bubble formed from 45 mm plastic sphere impacting stainless steel target. Every 10th image shown. The cavitation bubble pulses three times before becoming too small to resolve. The entire duration of the bubble pulses is approximately 2.2 ms.

A 45 mm diameter Ertacetal® plastic sphere attached to a thin rod was fitted to a spring-loaded mechanism that was mounted in the top of the BDC. A 100 mm diameter flat stainless steel target was located underneath the sphere. A trigger signal was used to simultaneously release the sphere and initialise high-speed recording of the cavitation bubble generated at impact. The photography was taken at 100 kHz using a LaVision HighSpeedStar8 camera, blacklit with a Dedocool light. The backlight was diffused through a 3 mm opaque white acrylic panel. DaVis 8.1 software was used to control the camera. The maximum bubble radius was measured from the images for static pressures ranging from 40 to 140 kPa and impact velocities of 1.3 to 3.2 m/s.

Results

Images from the high-speed photography, showing the development of the cavitation bubble on impact are shown in figure 3. The time shown upper right in each image corresponds to figure 4 which shows the sphere displacement and bubble radius growth. The sphere displacement, S, and bubble radius, r, are determined from the high-speed photography and non-dimensionalised on the sphere radius, r_s. The sphere displacement has been smoothed using a 5-point moving average filter.

The sphere impacts at t = 2.50 ms and the cavity generated undergoes rapid radial growth in the confined space between the sphere and the target. Small annular protrusions form towards the top and bottom of the bubble. At t = 2.85 the rebounding sphere reverses direction and moves towards the impact plate before the bubble reaches a maximum at about t = 2.97 ms. As the bubble starts to collapse the sphere pauses (t = 3.11 ms to 3.39 ms) before reversing direction again. As the sphere moves away from the plate the bubble is slightly drawn up (see image at t = 3.619 ms) before it reaches its first minimum at t = 3.74 ms. During the second growth, some nuclei activation occurs surrounding the bubble. The second bubble maximum occurs at t = 3.96 ms. Nuclei activation occurs again during the second collapse, with the second bubble minimum occurring at t = 4.27 ms. The bubble pulses a third time, with more nuclei activation, and then the main bubble becomes too small to resolve further pulses. The entire duration of the cavitation is approximately 2.2 ms.

Figure 4 shows the impact of the sphere on the target plate to occur after the appearance of the bubble. The sphere impacts

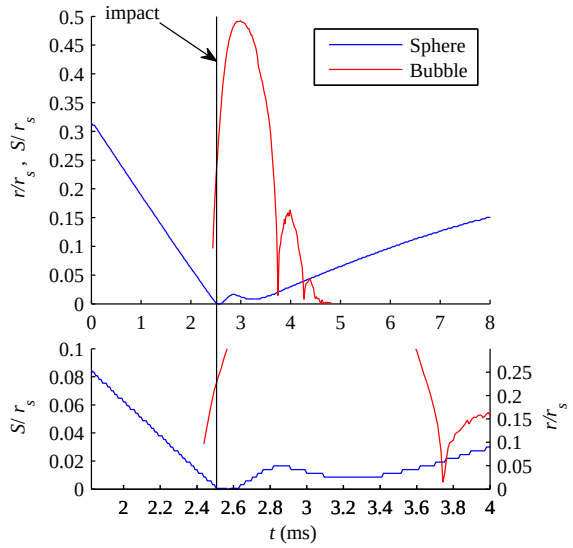

Figure 4. Sphere displacement, S, and bubble radius, r, with time. The bubble radius and sphere displacement are non-dimensionalised on the sphere radius, r_s. The first instance of the bubble occurs in frames preceding the minimum displacement of the sphere, suggesting that cavitation may occur before impact. Detailed view in bottom plot, where sphere displacement is not smoothed.

at frame 263 or t = 2.50476 ms. This frame, and two frames preceding this (258 and 260) are shown in figure 5. In this case the bubble is evident approximately 48 µs before the sphere has reached its point of rebound. It is possible that the sphere deforms slightly on impact, causing the body away from the centre point to continue downward displacement after the centre point has impacted the target. The potential sphere deformation requires further investigation; however, at this stage it appears that the bubble is indeed generated before impact. This is contrary to the claims of Mansoor *et al.* [4] who did not find evidence of cavitation until after impact and was in disagreement with claims by Seddon *et al.* [8] to have experimental evidence of the theories of Joseph [2].

Figure 6 shows the power law relationship between the maximum bubble radius and the cavitation number. The maximum bubble radius, r_{max}, is non-dimensionalised on the sphere ra-

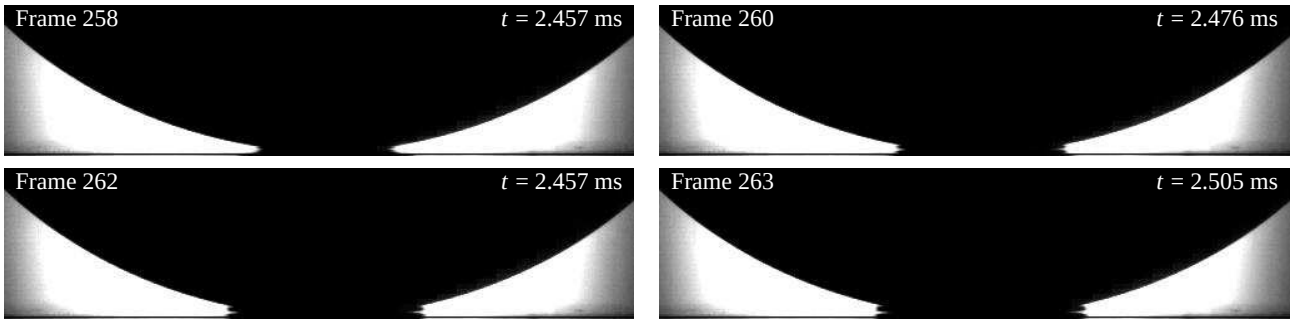

Figure 5. Images shown at frame 258 (top left), 260 (top right), 262 (bottom left) and 263 (bottom right). Frame 263 is the point of impact. The bubble is evident in the previous frames, suggesting that cavitation occurs before impact.

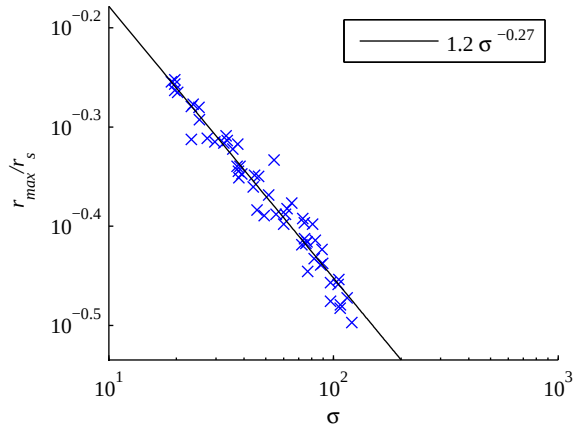

Figure 6. Maximum bubble radius vs. σ. Maximum bubble radius is non-dimensionalised on sphere diameter.

dius and the cavitation number, σ, is given by $(p - p_v)/\frac{1}{2}\rho U^2$ where p is the static test pressure, p_v is the water vapour pressure, ρ is the water density, and U is the sphere impact velocity. The impact velocity is calculated from the displacement over the period prior to impact. It was found that from the time the sphere entered the field of view, the velocity was constant until the point of impact.

Conclusions

The cavitation bubble generated when a plastic sphere impacts a stainless steel target plate has been captured using high-speed shadow photography. The maximum bubble radius is related to the cavitation number via a power law over the range of velocities and static pressures tested. There is evidence that the bubble is formed before the sphere impacts the target plate; however, further investigation into the deformations of the sphere at impact and greater temporal resolution are required in order to state this conclusively.

References

[1] Franc, J. and Michel, J., *Fundamentals of Cavitation*, Kluwer Academic Publishers, Dordrecht, The Netherlands, 2004.

[2] Joseph, D., Cavitation and the state of stress in a flowing liquid, *Journal of Fluid Mechanics*, **366**, 1998, 367–378.

[3] Lohse, D., Schmitz, B. and Versluis, M., Snapping shrimp make flashing bubbles, *Nature, Brief Communications*, **413**, 2001, 477–478.

[4] Mansoor, M., Uddin, J., Marston, J., Vakarelski, I. and S.T., T., The onset of cavitation during the collision of a sphere with a wetted surface, *Experiments in Fluids*, **55**, 2014, 1648 (7 pages).

[5] Marston, J., Vakarelski, I. and Thoroddsen, S., Bubble entrapment during sphere impact onto quiescent liquid surfaces, *Journal of Fluid Mechanics*, **680**, 2011, 660–670.

[6] Patek, S. and Caldwell, R., Extreme impact and cavitation forces of a biological hammer: strike forces of the peacock mantis shrimp *Odontodactylus Scyllarus*, *Journal of Experimental Biology*, **208**, 2005, 3655–3664.

[7] Patek, S., Korff, W. and Caldwell, R., Deadly strike mechanism of a mantis shrimp, *Nature*, **428**, 2004, 819–820.

[8] Seddon, J., Kok, M., Linnartz, E. and Lohse, D., Bubble puzzles in liquid squeeze: Cavitation during compression, *Europhysics Letters*, **97**, 2012, 24004 (5 pages).